

## Sensitivity of Avalanche Photodetector Receivers for Long-Wavelength Optical Communications

By R. G. SMITH and S. R. FORREST

(Manuscript received May 27, 1982)

*We consider, in detail, the potential improvement in receiver sensitivity that can be realized using an avalanche photodiode (APD) rather than the conventional p-i-n diode in long-wavelength optical communications systems. Numerical computations are used to determine optimum gains and receiver sensitivities for several values of ionization coefficient ratios and dark currents. Sensitivities are considered for transmission bit rates of 45 Mb/s, 90 Mb/s, and 274 Mb/s—values characteristic of present long-wavelength systems. We find that general relationships and scaling laws between receiver sensitivity and the other critical parameters can be formulated if the sensitivity is calculated in units relative to the quantum limit. An important result is that the improvement in APD sensitivity depends strongly on dark current, but only weakly on the ionization coefficient ratio. Our calculations are compared with recent results obtained for  $\text{In}_{0.53}\text{Ga}_{0.47}\text{As}/\text{InP}$  APDs sensitive in the  $\lambda = 0.95 \mu\text{m}$  to  $1.6 \mu\text{m}$  wavelength region. We also include a brief discussion comparing APD sensitivities with those obtained using phototransistors and majority carrier devices.*

### I. INTRODUCTION

In contrast to short wavelength ( $0.8 \mu\text{m}$  to  $0.9 \mu\text{m}$ ) lightwave transmission systems, which generally use an avalanche photodiode (APD) as the detection element,<sup>1</sup> many receivers for long wavelength ( $1.3 \mu\text{m}$  to  $1.55 \mu\text{m}$ ) lightwave systems use p-i-n detectors.<sup>2,3</sup> The principal reason for using the APD at short wavelengths is the  $\sim 15\text{-dB}$  improvement in sensitivity obtained compared with a p-i-n with a nonintegrating front end. The arguments given for using p-i-n's at long wavelengths are: (i) sensitivities comparable to those obtained at short

wavelengths can be achieved using GaAs field-effect transistor (FET) front-end amplifiers; (ii) the ionization coefficients for electrons and holes in InP and related InGaAsP compounds are not significantly different, leading to large excess noise factors and, hence, poor receiver sensitivities; and (iii) the APD is difficult to fabricate, especially with low dark currents.

In this paper the subject of receiver sensitivity using APDs is addressed with emphasis placed on the limits imposed by the ionization coefficients and the device dark currents. The principal result is that whereas the ratio of the ionization coefficients determines the maximum sensitivity improvement attainable with an APD, the degree to which this improvement can be achieved in practice is controlled by the dark current. It is concluded that, for sufficiently low dark currents, an APD can yield significant sensitivity improvements over that obtained using a p-i-n detector, resulting in greater regenerator spacings, or permitting the use of less sophisticated amplifiers with greater dynamic range and lower cost.

### **1.1 Detector alternatives**

In choosing a detector for lightwave receivers there are several alternatives to the p-i-n and APD, including the phototransistor,<sup>4,5</sup> majority carrier devices,<sup>6</sup> and photoconductors.<sup>7,8</sup> It has been claimed that these devices can produce gains comparable to, or in excess of, those attained with an APD but without the penalty of an excess noise factor. It is not, however, the value of an excess noise factor that is important, but rather the total noise contributed by the device in producing the associated gain. In contrast to the p-i-n and APD, which achieve high-speed operation under reverse bias, the phototransistor, the majority carrier detector, and the photoconductor all draw current when biased to obtain high-speed operation. These bias currents contribute significant noise to the receiver and limit the sensitivity. For the APD, dark currents also affect the sensitivity obtained but they are not, however, a necessary part of the high-speed operation, and can in principle be reduced to sufficiently low levels to achieve significant receiver sensitivity improvements.

### **1.2 Scope and organization**

In the material to follow, APD receiver sensitivities will be characterized with respect to bit rate, amplifier noise, ratio of ionization coefficients, and the detector dark current. The sensitivity improvement achieved as a function of the above parameters will be calculated and compared with recently reported results. The paper is organized as follows: in Section II we consider the base-line receiver sensitivity and develop the formalism for calculating sensitivity improvements

afforded with an APD. In Section III, we calculate the improvement obtained for an APD with zero dark current, and in Section IV we consider the effects of the dark current on degradation of the receiver sensitivity. In Section V, we present a general scaling rule for APD receiver sensitivity, and in Section VI we present sample calculations of receiver sensitivities of current interest, and compare the results of a recent measurement of a long-wavelength APD receiver sensitivity with our calculations. Finally, in Section VII, we present conclusions.

## II. RECEIVER SENSITIVITY

In analyzing the sensitivity of a digital receiver, we know that for a given decision level the net signal is a factor  $Q$  times the root-mean-square (rms) noise associated with the state transmitted<sup>9</sup> (mark or space), with  $Q = 6$  for a bit error rate (BER) of  $10^{-9}$ . For practical p-i-n detectors the noise is determined by the amplifier and the detector leakage currents, and is identical for both signal states. In this case the decision level is placed midway between the two signal levels and the sensitivity is given by

$$\eta \bar{P} = A \langle i^2 \rangle^{1/2}, \quad (1)$$

where  $\eta$  is the detector quantum efficiency including coupling losses,  $\bar{P}$  is the average optical power required to achieve a given BER, and  $\langle i^2 \rangle^{1/2}$  is the rms noise current of the receiver referred to the input. The parameter  $A$  is given by

$$A = Q \frac{h\nu}{q}, \quad (2)$$

where  $h\nu$  is the energy of the incident radiation and  $q$  is the electronic charge. For a BER =  $10^{-9}$ ,  $A = 9$  at  $\lambda = 0.825 \mu\text{m}$ , and  $A = 5.7$  at  $\lambda = 1.3 \mu\text{m}$ . Whereas the noise current,  $\langle i^2 \rangle$ , is normally used to characterize receivers, in the following calculations the total receiver sensitivity using a p-i-n detector will be used instead. The relation between the two quantities is given by eq. (1).

When an APD is used, both the signal current and the shot-noise associated with the signal current are multiplied by the avalanche process. For avalanche gains near the optimum value, the shot-noise associated with the signal is comparable to the receiver noise. Under these conditions the decision level, or threshold, is no longer midway between the two signal levels but is located closer to the space, or "0" level. Under the assumption that the received signal power is essentially zero in the off state (perfect source extinction), and that the detector dark current that undergoes multiplication is also zero, the receiver sensitivity is given by<sup>10</sup>

$$\eta\bar{P} = A \left[ \frac{\langle i^2 \rangle^{1/2}}{M} + (qBI_1)QF(M) \right], \quad (3)$$

where  $M$  is the average gain,  $B$  is the bit rate,  $I_1$  is a Personick integral  $\approx 0.5$ , and  $F(M)$  is the excess noise factor associated with the avalanche gain process. In deriving eq. (3), the optimum decision level has been assumed for each value of the gain  $M$ . In the limit  $M = 1$ , and neglecting the second term in brackets, which is small, eq. (3) is seen to reduce to eq. (1). In evaluating eq. (3) we use McIntyre's expression<sup>11</sup> for the excess noise factor,  $F(M)$ :

$$F(M) = M \left[ 1 - (1 - k) \left( \frac{M - 1}{M} \right)^2 \right]. \quad (4)$$

Here,  $k \leq 1$  is the ratio of the ionization coefficients of the ionizing carriers (holes or electrons) where it is assumed the avalanche is initiated by the carrier with the highest ionization rate.

Under more general circumstances of receiver operation the current produced by the optical source is not identically zero in the "0" level, nor is the detector dark current which undergoes multiplication necessarily negligible. Each source of current undergoing avalanche gain produces shot-noise that contributes to the total noise in both the "0" and "1" states. In general, the primary current should be less than approximately 10 percent of the photocurrent associated with the "1" state if its effect on sensitivity is to be small.

The effects of detector dark current can be handled by including both the unmultiplied and multiplied components as part of the receiver noise. Thus, the receiver noise becomes

$$\langle i^2 \rangle_{\text{total}} = \langle i^2 \rangle_a + 2qI_2B[I_{DU} + I_{DM}M^2F(M)], \quad (5)$$

where  $\langle i^2 \rangle_a$  is the amplifier noise independent of the detector leakage current,  $I_{DU}$  is the unmultiplied portion of the dark current,  $I_{DM}$  is the primary dark current, which undergoes avalanche gain, and  $I_2$  is a Personick integral,<sup>9,10</sup> which typically has a value between 0.5 and 0.6. In using eq. (5), it is assumed that the noise is Gaussian; also in the following treatment we assume that the detector dark current undergoes the same gain and has the same excess noise factor as the photo-generated current.

It can be shown that when detector dark current is considered, eq. (3) can be used to evaluate the sensitivity if  $\langle i^2 \rangle$  in eq. (3) is replaced with  $\langle i^2 \rangle_{\text{total}}$ , eq. (5). In this case the effective receiver noise is a function of the gain,  $M$ , with the result that simple analytical optimization of eq. (3) is difficult. In the calculations to follow, eq. (3), with the modification discussed above, has been numerically evaluated to find an optimum value of the gain. The results are obtained with the

assumption of complete source extinction. The effect of a nonideal source can be obtained by finding the equivalent extinction ratio corresponding to the assumed dark current and the primary signal current. Note also that, from eq. (5), the effect of unmultiplied dark currents such as surface leakage,  $I_{DU}$ , is in general not significant compared with the multiplied dark currents,  $I_{DM}$ . For example, in a receiver with an optimum gain of  $M = 10$ ,  $I_{DM} = 1$  nA contributes more to the total receiver noise than  $I_{DU} = 100$  nA (here  $F(M) \ll M$ ). Thus, in the remainder of this work we focus on the multiplied portion of the dark current, including  $I_{DU}$  in the basic amplifier noise.

### III. SENSITIVITY CALCULATIONS ( $I_{DM} = 0$ )

The sensitivity calculations to be presented here are given in detail for several bit rates of current interest. By normalizing sensitivities to the quantum limit it is shown that a universal sensitivity curve independent of bit rate can be derived. The parameters to be considered are the amplifier noise characterized by the equivalent receiver sensitivity, the effective ratio of ionization coefficients,  $k$ , and the primary dark current,  $I_{DM}$ , which undergoes multiplication.

Figure 1 is a plot of sensitivity at  $\lambda = 1.3 \mu\text{m}$  and 45 Mb/s for four values of  $k$  in the limit that the primary dark current is zero (perfect extinction of the source is assumed). The calculated sensitivities thus represent the best attainable values. Here  $\eta\bar{P}_{PIN}$  denotes the sensitivity of the amplifier using a p-i-n detector. Similarly, the vertical axis is the sensitivity of the same amplifier employing an APD. The numerical values in parentheses along each curve represent the optimum gain for the corresponding set of parameters. For example, in Fig. 1 a p-i-n receiver with a  $-50$  dBm sensitivity would have a sensitivity of  $-56.5$  dBm with an APD having  $k = 1$  at an optimum gain of  $M_{opt} \cong 9$ , and for  $k = 0.025$  the sensitivity improves to  $-62.3$  dBm at  $M_{opt} \cong 60$ . The p-i-n sensitivity of  $-50$  dBm is typical of that achievable with GaAs FET front ends,<sup>3</sup> while the assumed  $k$  values are typical<sup>12</sup> of Ge ( $k = 1$ ) and the best Si devices ( $k \cong 0.025$ ).

Several general features may be seen from these curves: Decreasing  $k$  results in a larger sensitivity improvement, and over the range of p-i-n sensitivities shown, the improvement achieved by the lowest  $k$ -value device is between 5 dB and 7 dB greater than the  $k = 1$  device. On the other hand, the improvement relative to a p-i-n afforded by the  $k = 1$  device is between 4.5 and 11.5 dB. Also, as the p-i-n receiver sensitivity increases, the improvement achieved with an APD diminishes. For  $k = 1$ , a 2-dB improvement in p-i-n sensitivity results in a 1-dB improvement for the same amplifier when using an APD. However, for  $k = 0.025$ , an improvement in p-i-n sensitivity of 3 dB is required to achieve the same 1-dB improvement when using an APD. Thus, the

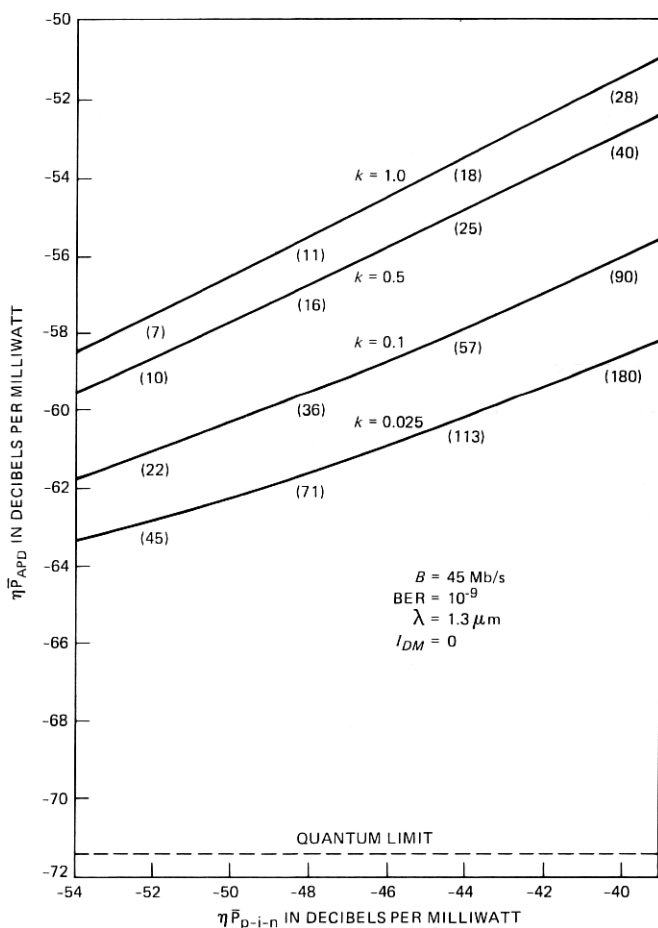


Fig. 1—APD sensitivity versus p-i-n sensitivity at a bit rate of 45 Mb/s and zero dark current ( $I_{DM}$ ), for several values of the ionization coefficient ratio,  $k$ . Numbers in parentheses indicate optimum gains yielding the corresponding value of APD sensitivity.

improvement to be gained with an APD diminishes as the amplifier performance is improved; conversely, the APD is more tolerant of poorer amplifier noise performance. Hence, an APD can permit the use of higher noise amplifiers, which in many cases, possess greater dynamic range. Another characteristic of APD receivers seen from Fig. 1 is that the optimum gain ( $M_{opt}$ ) decreases as  $k$  increases, and also  $M_{opt}$  decreases as the p-i-n sensitivity improves. For the range of parameters shown in the figure, the improvement afforded by an APD is between  $M_{opt}/2$  and  $M_{opt}/3$ .

Curves of sensitivity for bit rates of 90 Mb/s and 274 Mb/s are shown in Figs. 2 and 3, respectively. The range of p-i-n and APD

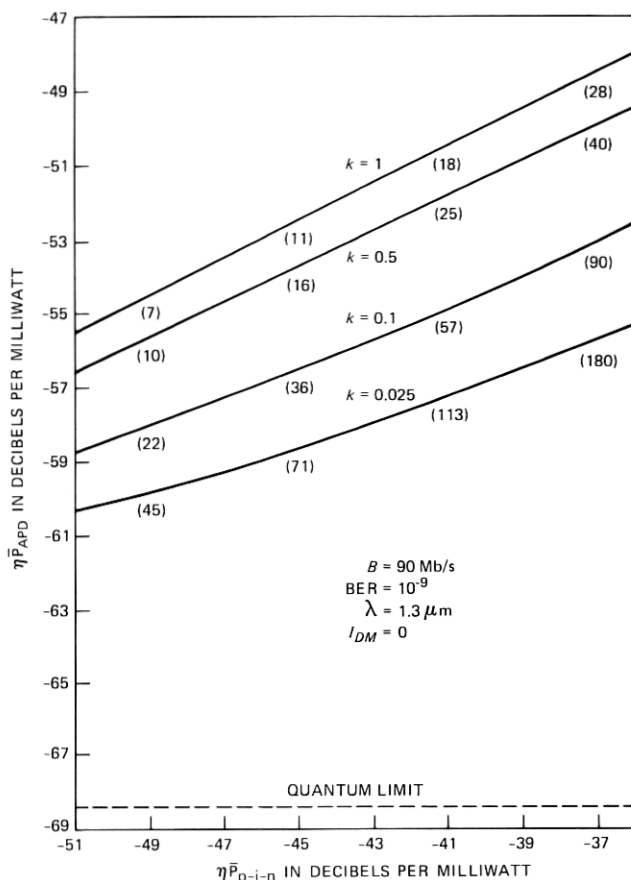


Fig. 2—Similar to Fig. 1 with  $B = 90 \text{ Mb/s}$ .

sensitivities covered by these curves are adjusted to include values that might be achieved at these different bit rates. Extrapolation to other bit rates can be made by noting that Figs. 1 to 3 are essentially identical except that the horizontal and vertical axes are scaled by a constant amount, dependent upon the bit rate. For example, Fig. 2 (for  $90 \text{ Mb/s}$ ) can be derived from Fig. 1 (for  $45 \text{ Mb/s}$ ) by adding  $3 \text{ dB}$  to both the ordinate and abscissa, e.g.,  $-50 \text{ dBm}$  at  $45 \text{ Mb/s}$  becomes  $-47 \text{ dBm}$  at  $90 \text{ Mb/s}$ , etc. This simple multiplicative scaling rule follows from eq. (3) and the method of defining the receiver noise in terms of the p-i-n sensitivity.

A curve applicable to all bit rates can be generated by defining all sensitivity values relative to the quantum limit,  $\eta \bar{P}_{QL}$ , which for a bit error rate of  $10^{-9}$ , is given by,

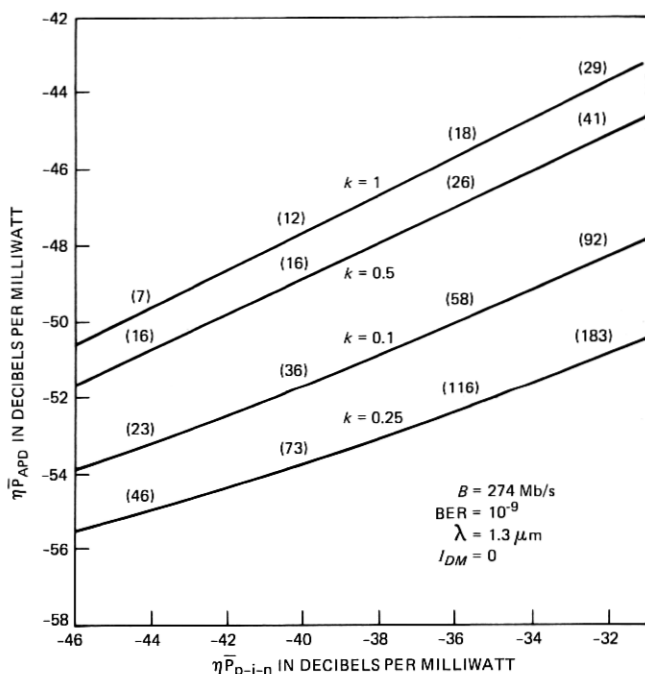


Fig. 3—Similar to Fig. 1 with  $B = 274$  Mb/s.

$$\eta \bar{P}_{QL} = \frac{21}{2} (h\nu) B. \quad (6)$$

This expression corresponds to 21 transmitted photons per mark, and a mark-to-space ratio of one. For  $\lambda = 1.3 \mu\text{m}$ , eq. (6) becomes

$$\eta \bar{P}_{QL} \text{ (dBm)} = -87.95 + 10 \log_{10} B \text{ (Mb/s)}. \quad (7)$$

Values of quantum limited sensitivity are plotted in Fig. 4.

Figure 5 is a universal plot of the improvement in sensitivity achieved with an APD with zero multiplied dark current and independent of bit rate for several values of  $k$ . The vertical axis is the improvement in sensitivity (in dB) achieved with an APD compared to a p-i-n using the same amplifier, while the horizontal axis is the difference between the sensitivity of the p-i-n receiver and the quantum limit. Again, the advantage provided by an APD is seen to diminish as the p-i-n sensitivity approaches the quantum limit. As an example, the current receiver designs using p-i-n/GaAs FET receivers have sensitivities typically in the range of 20 to 25 dB above the quantum limit.<sup>2,3</sup> The maximum sensitivity improvements afforded by an APD are thus greater than 6 dB for this range of p-i-n sensitivities, depending on the  $k$ -value.



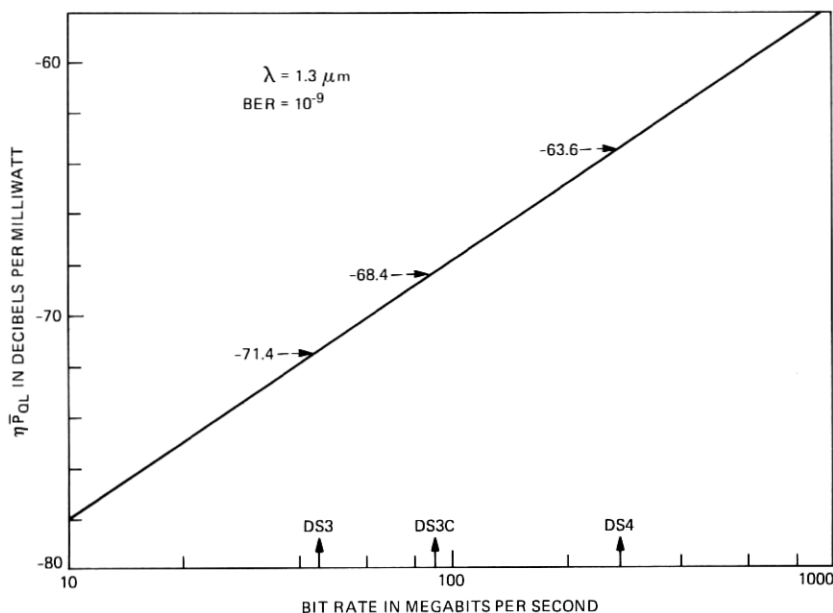


Fig. 4—Quantum limit ( $\eta\bar{P}_{QL}$ ) versus bit rate. Numbers indicate values for standard transmission system bit rates as labeled on the abscissa.

#### IV. SENSITIVITY CALCULATIONS ( $I_{DM} > 0$ )

The sensitivity improvements predicted above correspond to an ideal source and detector, in that the source extinction ratio is infinite and the dark current is negligible. In this section we investigate how much this improved performance is degraded by detector dark current. Since the absolute sensitivity depends upon dark current, the ratio of ionization coefficients, the receiver noise as characterized by the p-i-n sensitivity, and the bit rate, a large number of curves would have to be presented to discuss the full range of operating possibilities. Figures 6, 7, and 8 show the effect of primary dark current on sensitivity for bit rates of 45 Mb/s, 90 Mb/s, and 274 Mb/s. The p-i-n sensitivities indicated on each curve correspond to values currently achievable with optimized GaAs FET amplifiers. The arrows on the left-hand axis indicate the limiting sensitivity ( $I_{DM} = 0$ ) calculated in Section III above. The general features observed in these figures are the falloff of the sensitivity with increasing dark current, and the increased sensitivity to dark current as  $k$  decreases.

For example, at 45 Mb/s (Fig. 6),  $I_{DM} = 10^{-10}$  A reduces the maximum obtainable improvement for  $k = 0.025$  by  $\approx 1$  dB, while it has little impact for  $k = 1$ . At 90 Mb/s (Fig. 7) the same degradation for  $k = 0.025$  occurs for  $I_{DM} \approx 2 \times 10^{-10}$  A, and at 274 Mb/s (Fig. 8) it occurs for  $I_{DM} \approx 7 \times 10^{-10}$  A. Thus, at higher bit rates, the APD is tolerant of

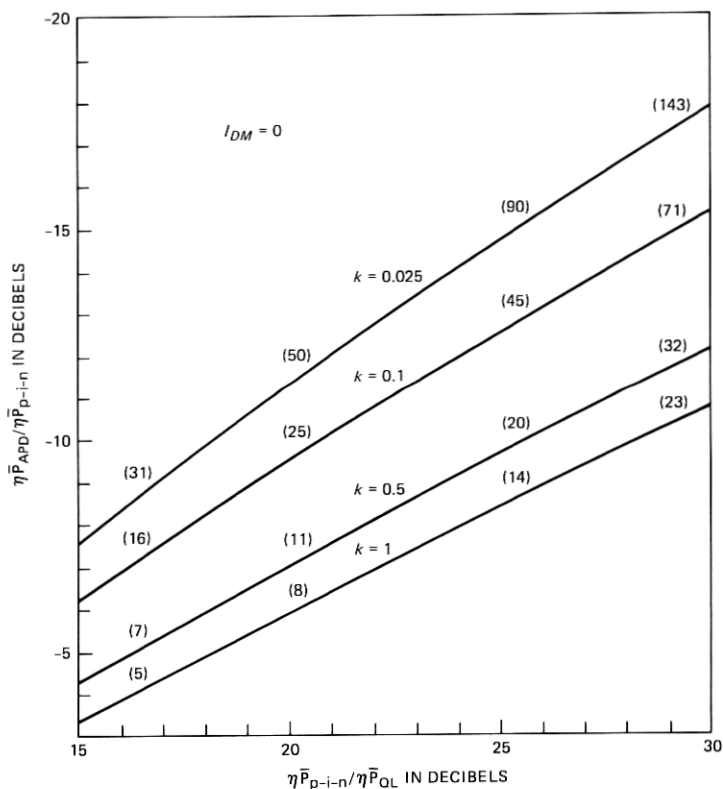


Fig. 5—Sensitivity improvement of the APD over p-i-n sensitivity versus normalized p-i-n sensitivity for zero dark current ( $I_{DM}$ ), and for several values of the ionization coefficient ratio,  $k$ . Numbers in parentheses indicate optimum APD gain. This plot is independent of bit rate.

greater dark current levels for equal sensitivity degradation. As we discuss below, the dark current producing a given degradation is directly proportional to the bit rate. A second feature of Figs. 6, 7, and 8 is that, whereas a lower  $k$ -value produces an improvement in sensitivity, the amount of improvement decreases with increasing primary dark current.

In a manner similar to that used to generate Fig. 5, a general curve, independent of bit rate, can be generated showing the effect of dark current on sensitivity. In Fig. 9 the p-i-n sensitivity is assumed to be 21.4 dB above the quantum limit, and the dark current normalized to the bit rate is expressed in nA/(Mb/s). The APD sensitivity relative to the quantum limit is shown on the left-hand axis, and the improvement afforded by the APD compared to the p-i-n is shown on the right-hand axis. Again, the rapid decrease in the advantage of an APD with increasing dark current is evident. Further, the advantage gained

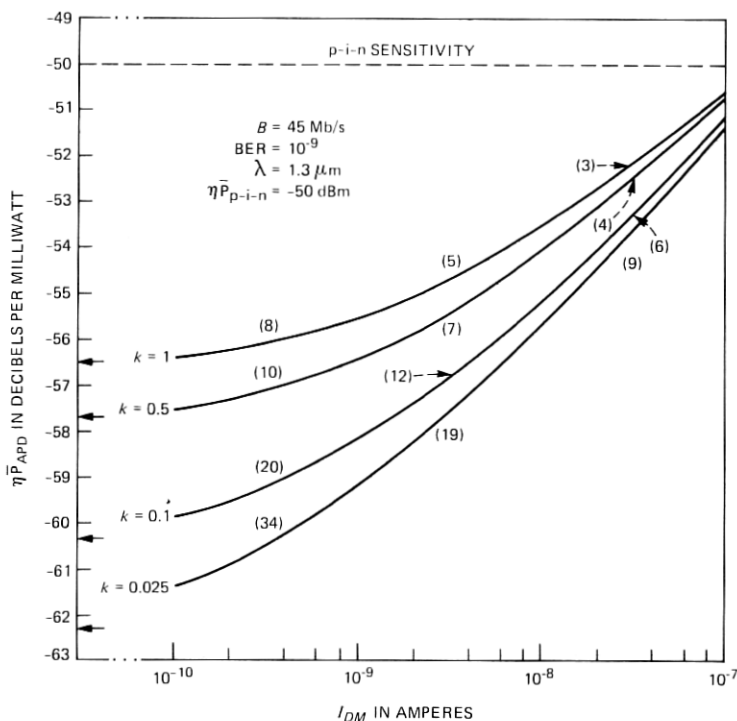


Fig. 6—APD sensitivity at 45 Mb/s versus primary dark current ( $I_{DM}$ ) for several values of the ionization coefficient ratio,  $k$ . Arrows along the vertical axis correspond to the APD sensitivity at  $I_{DM} = 0$ .

by using a low  $k$ -value APD compared to one with a larger  $k$  value is seen to be significant only when the dark currents are low, i.e., less than  $10^{-2} \text{ nA/Mb/s}$ .

The above calculations assume a p-i-n sensitivity very nearly equal to the best presently achievable. Figure 10 shows the effect of varying the p-i-n sensitivity. The figure is plotted for  $k = 0.5$ , a value typical of present  $\text{In}_{0.53}\text{Ga}_{0.47}\text{As/InP}$  APDs.<sup>13,14</sup> The left-hand and lower axes are plotted in normalized units, whereas the right-hand and upper axes are shown unnormalized for the three bit rates considered. The p-i-n sensitivities for each of the bit rates are shown in the box at the left. Included are values 3 dB better, and 3 dB and 6 dB worse than those used in the preceding calculations. From these curves we see that for low dark current values an improvement in p-i-n sensitivity by 3 dB results in a 1.4-dB improvement in APD sensitivity, whereas this value is decreased to  $\approx 1 \text{ dB}$  for the higher range of dark currents, i.e.,  $1 \text{ nA/(Mb/s)}$ . Similar curves can be generated for other values of  $k$  but will not be presented here.

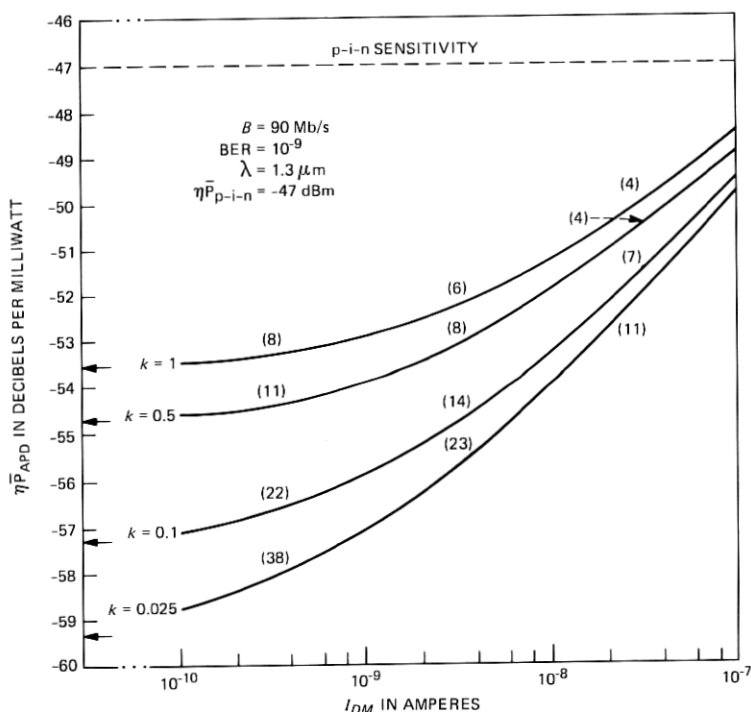


Fig. 7—Similar to Fig. 6 with  $B = 90$  Mb/s.

## V. GENERALIZED RELATION FOR ALLOWABLE DARK CURRENT

Because of the number of parameters involved in determining sensitivity, the preceding calculations have assumed a particular value for either the dark current,  $k$  value or p-i-n sensitivity. We now derive a relation between these quantities that defines the maximum allowable dark current for a given degradation of the sensitivity from the ideal ( $I_{DM} = 0$ ) case.

We begin by combining eqs. (1) to (3), (5), and (6) to give

$$\frac{\eta \bar{P}_{APD}}{\eta \bar{P}_{QL}} = \frac{\left[ \left( \frac{\eta \bar{P}_{p-i-n}}{\eta \bar{P}_{QL}} \right)^2 + \left( \frac{4}{7} \right)^2 \frac{I_{DM}}{qB} M^2 F \right]^{1/2}}{M} + \frac{12}{7} F. \quad (8)$$

In obtaining the numerical values in eq. (8), the Personick integrals  $I_1$  and  $I_2$  have both been set equal to 0.5, and we have used  $Q = 6$ . The unmultiplied dark current,  $I_{DU}$ , is included in the p-i-n sensitivity. This expression is independent of bit rate provided  $I_{DM}/B$  is constant. Minimizing eq. (8) with respect to  $M$  in the limit  $I_{DM} = 0$ , and using eq. (4) for  $F$  gives the results presented in Fig. 5. Defining

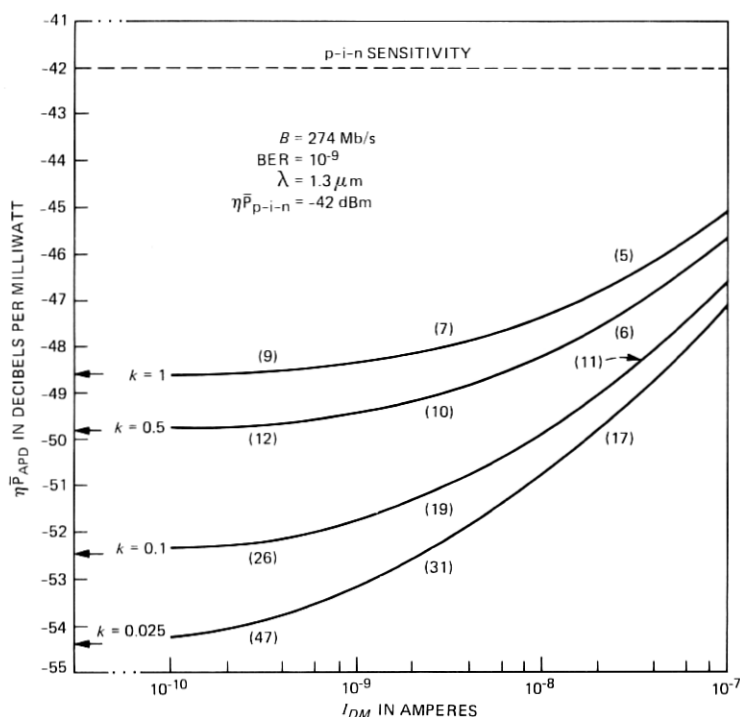


Fig. 8—Similar to Fig. 6 with  $B = 274 \text{ Mb/s}$ .

$$R = \frac{\eta \bar{P}_{p-i-n}}{\eta \bar{P}_{QL}}, \quad (9)$$

the optimum gain,  $M_{\text{opt}}$ , for  $I_{DM} = 0$  is then given by

$$M_{\text{opt}} = \left( \frac{7}{12} R + k - 1 \right)^{1/2} / k^{1/2}. \quad (10)$$

In this limit eqs. (8) to (10) yield

$$\left( \frac{\eta \bar{P}_{APD}}{\eta \bar{P}_{QL}} \right)_{I_{DM}=0} = \frac{24}{7} (k M_{\text{opt}} + 1 - k). \quad (11)$$

If the APD sensitivity is now degraded by some amount, for example by 1 dB because of non-zero dark current, eqs. (8) and (11) can be combined to define the locus of gains,  $M$ , and normalized dark currents,  $I_{DM}/qB$ , yielding that degradation. The maximum value of  $I_{DM}/qB$  for which a positive real value of  $M$  exists then defines the maximum value of the normalized dark current for which the degraded sensitivity can be obtained. Figure 11 shows a plot of the normalized dark current that results in a 1-dB degradation from the ultimate attainable im-

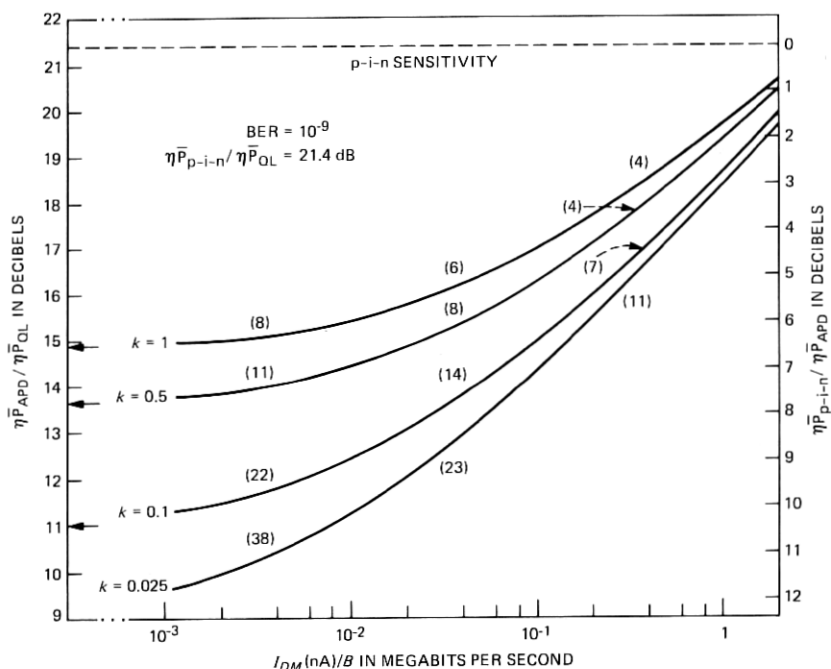


Fig. 9—APD sensitivity referred to the quantum limit versus primary dark current ( $I_{DM}$ ) per bit rate ( $B$ ) for several values of the ionization coefficient ratio,  $k$ . Numbers in parentheses indicate the optimum gains needed to achieve the corresponding APD sensitivities. Arrows along the vertical axis correspond to the APD sensitivity obtained at  $I_{DM} = 0$ .

provement ( $I_{DM} = 0$ ). As an example, a receiver with a p-i-n sensitivity 20 dB above the quantum limit and with  $k = 0.5$  will suffer a 1-dB degradation at  $I_{DM}/qB \cong 1.4 \times 10^{-2}$  nA/Mb/s. At a bit rate of 45 Mb/s, this corresponds to a primary dark current of  $\approx 0.6$  nA. On the other hand, at 274 Mb/s the same degradation would result for  $I_{DM} \approx 4$  nA. For a Si detector with  $k \approx 0.025$ , the primary dark currents yielding a 1-dB degradation would be a factor of six lower in each case. From Fig. 11 we see that the maximum permissible dark current decreases as the p-i-n receiver sensitivity increases and also as the  $k$ -value is decreased. Since the curves in Fig. 11 are nearly straight and parallel lines, they can be fit by a simple, approximate relation accurate to better than 20 percent over practical values of  $R$  and  $k$ . Therefore,

$$I_{DM}(\text{nA}) \approx 2 \times 10^{-3} (Rk)^{1/2} B \text{ (Mb/s)} \quad (12)$$

for a 1-dB penalty. Thus, an improvement in p-i-n sensitivity by a factor of 4, or a decrease of  $k$  by a factor of 4, would result in a reduction in the maximum allowable dark current by a factor of 2.

The above relation and Fig. 11 are for a degradation in sensitivity of

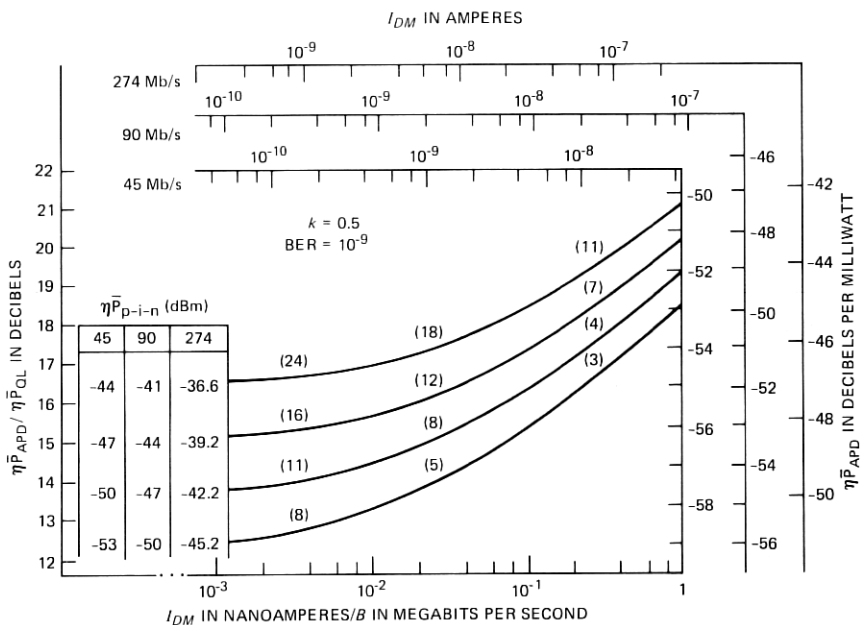


Fig. 10—Similar to Fig. 9 with  $k = 0.5$  for several values of p-i-n receiver sensitivity ( $\eta \bar{P}_{p-i-n}$ ) and bit rate.

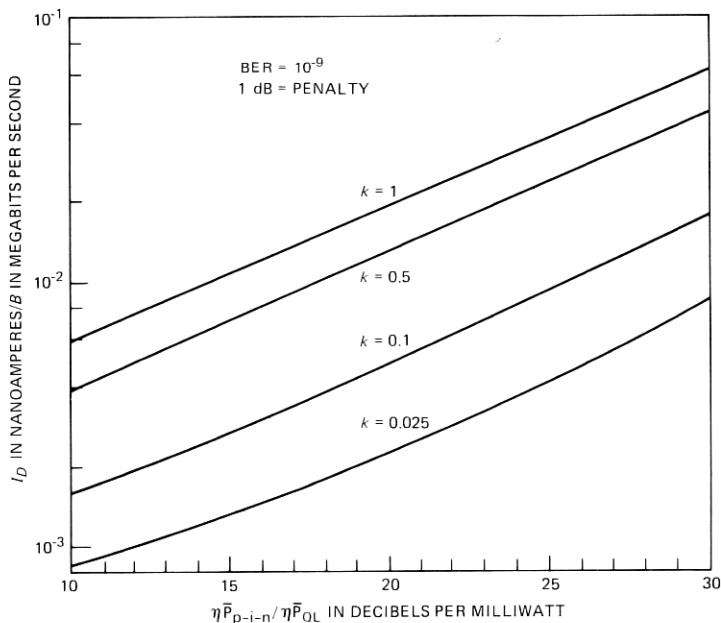


Fig. 11—Allowable primary APD dark current ( $I_{DM}$ ) per bit rate ( $B$ ) resulting in a 1-dB penalty from ultimately attainable APD sensitivity, as a function of p-i-n receiver sensitivity normalized to the quantum limit. Plots for several values of the ionization coefficient ratio,  $k$ , are shown.

1 dB. For a degradation in sensitivity of 2 dB, the corresponding primary dark current values are increased by a factor of 3.4.

## VI. EXAMPLES

Using the above results, we calculate the expected sensitivity improvements that might be obtained and the dark current limitations for several possible bit rates. We consider a p-i-n receiver yielding a sensitivity of 20 dB above the quantum limit (-51.4 dBm at 45 Mb/s, -48.4 dBm at 90 Mb/s, and -43.6 dBm at 274 Mb/s). This value lies between values achieved to date and those achievable assuming circuit improvements. We consider both  $k = 0.5$  and 0.1 values typical of present devices,<sup>13,14</sup> as well as more sophisticated structures.<sup>15</sup>

Table I gives the maximum permissible dark current as a function of bit rate at which point the sensitivity values are degraded by 2 dB from the ideal, i.e., 5-dB net improvement for  $k = 0.5$ , and 7.5-dB net improvement for  $k = 0.1$  (see Fig. 5). As we see in Table I, the permissible current values increase with bit rate, and decrease by a factor  $\approx 2$  for a reduction by a factor of 5 in  $k$ . Whereas the values in Table I are comparable to dark current values presently attainable,<sup>13,16</sup> it is noted that these are maximum values, and hence correspond to dark currents obtained at the highest operating temperature of the device. For a maximum temperature of 70°C typical of most system requirements, the increase in dark current compared to room temperature is typically a factor of 8.<sup>17</sup> Hence, if the detector is to operate under the assumed conditions, the room temperature dark currents must be a factor of 8 below the values shown in Table I, i.e., 250 pA for a 45-Mb/s system and  $k = 0.5$ .

We now compare our calculations to recent measurements of sensitivity made on a long-wavelength  $\text{In}_{0.53}\text{Ga}_{0.47}\text{As}/\text{InP}$  APD receiver. In the measurement of Forrest et al.,<sup>13</sup> at  $B = 45$  Mb/s, an APD receiver sensitivity of  $\eta \bar{P}_{APD} = -53.2$  dBm and at  $k \approx 0.5$  was reported. At this bit rate, Fig. 10 gives  $I_{DM} = 2.5$  nA at the measurement temperature of 20°C. The diode area was  $A = 1.3 \times 10^{-4}$  cm<sup>2</sup>. For detectors presently being considered, a reduced area of  $A \approx 5 \times 10^{-5}$  cm<sup>2</sup> would in turn reduce the bulk current to  $I_{DM} \approx 1$  nA at 20°C. Thus, at a maximum operating temperature of 70°C, we expect  $I_{DM} \approx 8$  nA. In Table II we

Table I—Maximum primary dark current (nA) giving a 2-dB degradation in APD sensitivity

Bit Rate (Mb/s)	$k = 0.5$	$k = 0.1$
45	2	0.8
90	4	1.5
274	12	4.5



Table II—Improvement in receiver sensitivity (in dB) using a state-of-the-art APD with  $I_{DM} = 8$  nA at 70°C and  $k = 0.5$

$\eta \bar{P}_{pin}(\text{dBm})$	$B(\text{Mb/s})$		
	45	90	274
-50	4.3*	3.1	1.9
-47	6.3	5.1*	3.6
-42	9.6	8.6	6.4*

\* Numbers refer to state-of-the-art receiver sensitivities at corresponding bit rates.

Table III—Improvement in receiver sensitivity using an APD with  $I_{DM} = 800$  pA at 70°C and  $k = 0.5$

$\eta \bar{P}_{pin}(\text{dBm})$	$B(\text{Mb/s})$		
	45	90	274
-50	6.5*	5.1	3.0
-47	8.5	7.1*	4.7
-42	11.5	9.7	7.5*

\* Numbers refer to state-of-the-art receiver sensitivities at corresponding bit rates.

show the improvement in receiver sensitivity afforded by this APD at several values of bit rate and receiver sensitivities. As is evident, the improvement increases with bit rate and with increasing receiver noise. For comparison, in Table III we show the sensitivity improvement if the APD dark current were reduced by a factor of ten (i.e., 100 pA at 20°C or 800 pA at 70°C).

## VII. CONCLUSIONS

We have calculated the improvement in sensitivity of receivers employing a long-wavelength avalanche photodiode rather than the traditionally used p-i-n detectors. The calculations consider receivers operating at bit rates of 45 Mb/s, 90 Mb/s, and 274 Mb/s, and sensitivities have been calculated for a wide range of  $I_{DM}$  and  $k$  values. We have found a strong degradation of receiver sensitivity with increasing APD dark current, with a much weaker dependence of sensitivity on the ionization coefficient ratio,  $k$ . Indeed, to fully realize the potential of APD's based on InP heterostructures, a considerable reduction in presently attainable dark currents is required.

## REFERENCES

1. R. G. Smith, C. A. Brackett, and H. W. Reinbold, "Optical Detector Package," B.S.T.J., 57, No. 6 (July-August 1978), pp. 1809-22.

2. D. R. Smith, R. C. Hooper, K. Ahmad, D. Jenkins, A. W. Mabbitt, and R. Nicklin, "p-i-n/F.E.T. Hybrid Optical Receiver for Longer-Wavelength Optical Communication Systems," *Electron. Lett.*, **16** (January 1980), pp. 69-71.
3. D. Gloge, A. Albanese, C. A. Burrus, E. L. Chinnock, J. A. Copeland, A. G. Dentai, T. P. Lee, Tingye Li, and K. Ogawa, "High-Speed Digital Lightwave Communication Using LEDs and PIN Photodiodes at 1.3  $\mu\text{m}$ ," *B.S.T.J.*, **59**, No. 8 (October 1980), pp. 1365-82.
4. D. Fritzsche, E. Kuphal, and R. Aulbach, "Fast Response InP/InGaAsP Heterojunction Phototransistors," *Electron. Lett.*, **17**, No. 5 (March 1981), pp. 178-80.
5. J. C. Campbell, C. A. Burrus, A. G. Dentai, and K. Ogawa, "Small-Area High-Speed InP/InGaAs Phototransistor," *Appl. Phys. Lett.*, **39**, No. 10 (November 15, 1981), pp. 820-1.
6. C. Y. Chen, A. Y. Cho, P. A. Garbinski, C. G. Bethea, and B. F. Levine, "Modulated Barrier Photodiode: A New Majority-Carrier Photodetector," *Appl. Phys. Lett.*, **39**, No. 4 (August 15, 1981), pp. 340-2.
7. J. Barnard, H. Ohno, C. E. C. Wood, and L. F. Eastman, "Integrated Double Heterostructure  $\text{Ga}_{0.47}\text{In}_{0.53}\text{As}$  Photoreceiver With Automatic Gain Control," *IEEE Electron. Dev. Lett.*, **EDL-2**, No. 1 (January 1981), pp. 7-9.
8. J. Degani, R. F. Leheny, R. E. Nahory, M. A. Pollack, J. P. Heritage, and J. C. DeWinter, "Fast Photoconductive Detector Using p- $\text{In}_{0.53}\text{Ga}_{0.47}\text{As}$  With Response to 1.7  $\mu\text{m}$ ," *Appl. Phys. Lett.*, **38** (January 1981), pp. 27-9.
9. S. D. Personick, "Receiver Design for Digital Fiber Optic Communication Systems I," *B.S.T.J.*, **52**, No. 6 (July-August 1973), pp. 843-74.
10. R. G. Smith and S. D. Personick, "Receiver Design for Optical Fiber Communication Systems," *Topics in Applied Physics*, **39**, H. Kressel, Ed., Berlin: Springer-Verlag, 1979, pp. 89-160.
11. R. J. McIntyre, "Multiplication Noise in Uniform Avalanche Diodes," *IEEE Trans., Electron. Dev.* **ED-13** (January 1966), pp. 164-8.
12. G. E. Stillman and C. M. Wolfe, "Avalanche Photodiodes," *Semiconductors and Semimetals*, **12**, Willardson and Beers, Ed., New York: Academic Press.
13. S. R. Forrest, G. F. Williams, O. K. Kim, and R. G. Smith, "Excess-Noise and Receiver Sensitivity Measurements of  $\text{In}_{0.53}\text{Ga}_{0.47}\text{As}$ /InP Avalanche Photodiodes," *Electron. Lett.*, **17**, No. 24 (November 1981), pp. 917-9.
14. N. Susa, H. Nakagome, O. Mikami, H. Ando, and H. Kanbe, "New InGaAs/InP Avalanche Photodiodes Structure for the 1-1.6  $\mu\text{m}$  Wavelength Region," *IEEE J. Quant. Electron.*, **QE-16**, No. 8 (August 1980), pp. 864-9.
15. F. Capasso, W. T. Tsang, A. L. Hutchinson, and G. F. Williams, "Enhancement of Electron Impact Ionization in a Superlattice: A New Avalanche Photodiode With a Large Ionization Rate Ratio," *Appl. Phys. Lett.*, **40**, No. 1 (January 1, 1982), pp. 38-40.
16. O. K. Kim, S. R. Forrest, W. A. Bonner, and R. G. Smith, "A High Gain  $\text{In}_{0.53}\text{Ga}_{0.47}\text{As}$ /InP Avalanche Photodiode With No Tunneling Leakage Current," *Appl. Phys. Lett.*, **39** (September 1981), pp. 402-4.
17. S. R. Forrest, R. F. Leheny, R. E. Nahory, and M. A. Pollack, " $\text{In}_{0.53}\text{Ga}_{0.47}\text{As}$  Photodiodes With Dark Current Limited by Generation-Recombination and Tunneling," *Appl. Phys. Lett.*, **37** (August 1980), pp. 322-5.